EPR Study of the $[Fe_4S_4]^+$ State in Single Crystals of $(Et_4N)_3[Fe_4S_4(SCH_2Ph)_4]$: g-Tensors of Kramers Doublets of the $S = {}^3/_2$ Ground State

Jocelyne Gloux[†] and Pierre Gloux*[,‡]

Contribution from the CEA/Département de Recherche Fondamentale sur la Matière Condensée, SESAM/SCPM, 38054 Grenoble Cedex 9, France

Received December 12, 1994[⊗]

Abstract: Electron paramagnetic resonance (EPR) of single crystals of the synthetic compound $(Et_4N)_3[Fe_4S_4(SCH_2Ph)_4]$ is presented. The measurements had to be done at very low temperature (a few kelvins) to avoid broadening of the EPR lines by the fast spin–lattice relaxation. Broadening and splittings of the lines result nevertheless from the spin–spin interactions between the paramagnetic $[Fe_4S_4]^+$ "cubanes". However, one can follow the EPR lines of the transitions within the fundamental and excited Kramers doublets associated with the effective spin $S = {}^3/_2$ of the ion $[Fe_4S_4]^+$. The two corresponding effective g-tensors are associated with a strongly nonaxial zero field splitting tensor ($\lambda \cong {}^1/_3$) and real g values around $g_{av} = 1.9$. These results are discussed in relation to the theories of strong double exchange.

Introduction

An important family of metalloproteins is that of the iron–sulfur proteins in which the active site involves one or several irons, formally Fe^{2+} or Fe^{3+}, generally tetrahedrally coordinated with the sulfurs. In the 4Fe-4S proteins in particular, there exists an active site Fe_4S_4 having a cubane type structure. It is found in three charge states: (i) $[Fe_4S_4]^+$ in the reduced ferredoxins, formally one Fe^{3+} for three Fe^{2+}; (ii) $[Fe_4S_4]^{2+}$ in the oxidized ferredoxins and in the reduced HiPIP, formally two Fe^{3+} for two Fe^{2+}; and (iii) $[Fe_4S_4]^{3+}$ in the oxidized HiPIP, formally three Fe^{3+} for one Fe^{2+}.[1] The research in biology on the active sites of proteins is accompanied by work in the synthesis chemistry of model compounds with the object of simulating these active sites. Holm and co-workers have synthesized 4Fe-4S groups of the cubane type: the $[Fe_4S_4]^+$ type in the compounds $(R'_4N)_3[Fe_4S_4(SR)_4]$ and the $[Fe_4S_4]^{2+}$ type in the compounds $(R'_4N)_2[Fe_4S_4(SR)_4]$.[2] On the other hand, only one synthesis of the $[Fe_4S_4]^{3+}$ type is known.[3]

Electron paramagnetic resonance (EPR) is a powerful physical method for studying a ground state with spin, as is the case a priori for the "cubanes" $[Fe_4S_4]^+$ or $[Fe_4S_4]^{3+}$ which have an odd number of electrons. In these Fe-S structures where the iron ions are in tetrahedral coordination with the ligands, the ligand field is assumed to be sufficiently weak to lead to high-spin situations, that is to local (i.e. individual) spins $S = {}^5/_2$ (ferric case) and $S = 2$ (ferrous case), but because of the coupling between the spins of the individual irons, the spins observed in the proteins or in the model compounds by EPR of frozen solutions or powders are not these local spins but total spins that are generally smaller. The $[Fe_4S_4]^{3+}$ type always has spin $S = {}^1/_2$.[4,5] The $[Fe_4S_4]^+$ type generally has spin $S = {}^1/_2$ in the proteins (even if it is found sometimes with spin $S = {}^3/_2$ or higher)[4,6] but often has spin $S = {}^3/_2$ in the model compounds.[7] On the other hand, with an even number of electrons, the $[Fe_4S_4]^{2+}$ type is diamagnetic ($S = 0$).

It is now generally accepted that these complexes involve weak interactions between the transition metals. Theoretical calculations of energy levels and orbitals, in particular magnetic orbitals, are developed within this framework by density-functional methods.[8] In a parallel direction, spin Hamiltonians which could describe the couplings between local spins that lead to the total spins actually observed are investigated. To explain the presence of a total spin smaller than the local spins, it is reasonable to consider that antiferromagnetic Heisenberg couplings occur. Indeed, authors of the earliest models essentially invoked couplings of this kind.[9,10] However, recent years have seen the introduction of a resonance integral for mixed-valence pairs Fe^{2+}–Fe^{3+} that, from the orbital point of view, leads to the delocalization of the 11th d-electron. In the spin Hamiltonian, this integral finds expression in the interaction called double exchange, linear in the pair spin quantum number.[11]

Of course, these theoretical models can be improved only by comparison with experiments providing sufficient experimental parameters. In the framework of EPR spectroscopy and of related spectroscopic techniques such as ENDOR, if the studies are limited to frozen solutions of proteins and to powders

* Author to whom correspondence should be addressed.
† Also at the University Joseph Fourier, Grenoble.
‡ Also with CNRS, Grenoble.
⊗ Abstract published in *Advance ACS Abstracts*, July 1, 1995.

(1) Lovenberg, W., Ed. *Iron-Sulfur Proteins*; Academic Press: New York, 1977; Vol. III.
(2) Berg, J. M.; Holm, R. H. In *Metal Ions in Biology*; Spiro, T. G., Ed.; Interscience: New York, 1982; Vol. 4, Chapter 1.
(3) O'Sullivan, T.; Millar, M. M. *J. Am. Chem. Soc.* **1985**, *107*, 4096.
(4) Cammack, R., Ed. Iron-Sulfur Proteins. In *Advances in Inorganic Chemistry*; Sykes, A. G., Ed.; Academic Press: New York, 1992; Vol. 38.
(5) Papaefthymiou, V.; Millar, M. M.; Münck, E. *Inorg. Chem.* **1986**, *25*, 3010.
(6) High spin states are found in selenium-substituted 4Fe-4Se ferredoxins: Gaillard, J.; Moulis, J.-M.; Auric, P.; Meyer, J. *Biochemistry* **1986**, *25*, 464.
(7) (a) Carney, M. J.; Papaefthymiou, G. C.; Spartalian, K.; Frankel, R. B.; Holm, R. H. *J. Am. Chem. Soc.* **1988**, *110*, 6084. (b) Carney, M. J.; Papaefthymiou, G. C.; Frankel, R. B.; Holm, R. H. *Inorg. Chem.* **1989**, *28*, 1497.
(8) Noodleman, L.; Case, D. A. In *Advances in Inorganic Chemistry*; Sykes, A. G., Ed.; Academic Press: New York, 1992; Vol. 38, p 423.
(9) Middleton, P.; Dickson, D. P. E.; Johnson, C. E.; Rush, J. D. *Eur. J. Biochem.* **1978**, *88*, 135.
(10) (a) Papaefthymiou, G. C.; Laskowski, E. J.; Frota-Pessoa, S.; Frankel, R. B.; Holm, R. H. *Inorg. Chem.* **1982**, *21*, 1723. (b) Collison, D.; Mabbs, F. E. *J. Chem. Soc., Dalton Trans.* **1982**, 1565.
(11) (a) Noodleman, L.; Baerends, E. J. *J. Am. Chem. Soc.* **1984**, *106*, 2316. (b) Münck, E.; Papaefthymiou, V.; Surerus, K. K.; Girerd, J.-J. In *Metal Clusters in Proteins*; Que, L., Jr., Ed.; ACS Symposium Series 372; American Chemical Society: Washington, DC, 1988. (c) Bominaar, E. L.; Borshch, S. A.; Girerd, J.-J. *J. Am. Chem. Soc.* **1994**, *116*, 5362.

0002-7863/95/1517-7513$09.00/0

and frozen solutions for the model compounds, all of the directional parameters escape analysis; for instance, for an effective g-tensor only the effective g values are accessible, the principal directions remaining unknown. In recent years, our group has developed research aiming at the measurement of these directional parameters in the case of 4Fe-4S synthetic cubanes. One original approach that we have adopted consists of using γ-irradiated single crystals of $[Fe_4S_4]^{2+}$ diamagnetic compounds. This has allowed creation of species of the $[Fe_4S_4]^{+}$ and $[Fe_4S_4]^{3+}$ types and then determination of the complete effective g-tensors of these species within the diamagnetic matrix for several compounds,[12] as well as determination of hyperfine tensors of the Fe^{57} nuclei[13] and of the protons.[14] Also, these species present the advantage of having a low concentration, which avoids the spectroscopic complications due to the spin−spin interactions between the paramagnetic centers.

All of the species $[Fe_4S_4]^{+}$ and $[Fe_4S_4]^{3+}$ created in $[Fe_4S_4]^{2+}$ by γ-irradiation have spin $S = {}^1/_2$ only. To do single-crystal EPR studies for the case of a spin $S = {}^3/_2$, it is therefore necessary to study the *intrinsic* species $[Fe_4S_4]^{+}$ that have been synthesized, although, as we shall see afterward, the experimental difficulties are greater and, moreover, the spectra are complicated by the presence of spin−spin interactions. This provides the advantage that the geometry of the paramagnetic species itself is available. We shall notice that the interest of single-crystal EPR studies is reinforced in the case of a spin $S = {}^3/_2$ compared with a spin $S = {}^1/_2$ by the fact that powder EPR may give less information for a spin $S = {}^3/_2$ than for a spin $S = {}^1/_2$. In these compounds the spin $S = {}^3/_2$ multiplets occur in the form of two Kramers doublets, to which specific effective g-tensors correspond. However, in the majority of cases powder EPR has only given the effective g values of the ground doublet, whereas using single-crystal EPR, we can hope to obtain information about the effective g-tensors of the fundamental and excited doublets of a spin $S = {}^3/_2$.

It appears that the $S = {}^3/_2$ spin state is important in the species $[Fe_4S_4]^{+}$ of synthetic compounds, whereas the spin ${}^1/_2$ state is usually found for the same species in proteins. Carney et al.,[7] using various physical methods—Mössbauer effect, magnetic susceptibility, and in particular powder EPR—have examined the various ground spin states found in the species $[Fe_4S_4]^{+}$ of synthetic compounds and classed them in three categories: pure spins $S = {}^3/_2$ (and one case of spin $S = {}^1/_2$), physical mixtures of pure spins $S = {}^3/_2$ and $S = {}^1/_2$, and quantum mixtures of pure spins $S =$ "${}^3/_2 + {}^1/_2$". One example of the last category has been particularly well documented, the spin of the cubane $[Fe_4S_4]^{+}$ of the compound $(Et_4N)_3[Fe_4S_4(SCH_2Ph)_4]$. The work that we present below is devoted to single-crystal EPR in this compound, to the study of the fundamental and excited Kramers doublets, and to their relation with the geometry of the cubane and with the theoretical models. To our knowledge, this is the first study of an intrinsic spin by single-crystal EPR in the iron−sulfur synthetic compounds.

EPR Spectroscopy

The compound is prepared following the single-step synthesis method of Hagen et al.[15] Recrystallization from acetonitrile leads to crystals which develop in the space group Cc of the monoclinic system,[16] generally in the shape of thin plates bc of which one edge is the axis **b**. These crystals are stored in a glovebox to avoid their oxidation, which would produce signal decrease and parasite signals. EPR measurements of the second derivative of the absorption were done on a Varian E-109 X band spectrometer equipped with a helium variable temperature device from Oxford Instruments. In this compound the line broadening by spin−lattice relaxation is such that already at 10−12 K the lines are hardly observable. Consequently, the experiments were generally done at very low temperature, near 4 K.

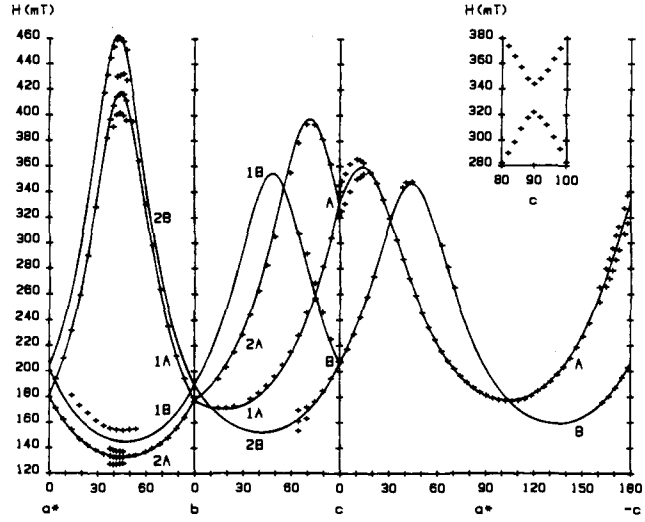

Figure 1. Experimental points and fitted angular variations of the resonance fields for the Kramers doublets A and B in the three orthogonal planes a^*b, bc, and ca^*. The curves are labeled 1 for the EPR site of Table 1 and 2 for the second EPR site. The inset details the ±10° range around **c** in the plane bc for doublet A, showing the noncrossing behavior of the data points corresponding to the two EPR sites. Microwave frequency is 9.231 GHz. The splittings by spin−spin interaction, not considered in the fit, are not shown in the graph of the angular variations.

The crystalline thin plates about 1 mm × 2 mm were held with grease on a plate of plexiglass which could be set on the sample holder in three different ways so that the magnetic field describes three planes perpendicular to each other in the crystal. To study the three orthogonal basic planes a^*b, bc, and ca^*, the crystalline plate bc was laid down on the plexiglass plate with edge **b** placed against a shoulder. The correct positions of both plane bc on the plexiglass plate and edge **b** against the shoulder were particularly crucial given that a small disorientation had a notable effect on the line positions on account of the strong anisotropy of the couplings. The extreme fragility of the single crystals made manipulating them to remedy a possible disorientation particularly delicate. Moreover, the reference elements, namely the plane bc and the edge **b**, were not perfect. We had to repeat our experiments many times before obtaining angular variations of the EPR transitions that we believed to be reliable because reproducibility in the three basic planes a^*b, bc, and ca^*. These angular variations are plotted in Figure 1, where the transitions are identified by the corresponding resonance fields in millitesla; points represent the experimental data, and continuous lines correspond to the subsequent fit. The orientation of axes in the plane ca^* has been identified on samples where the direction of the **a** axis in the plane ca^* was

(12) (a) Gloux, J.; Gloux, P.; Lamotte, B.; Rius, G. *Phys. Rev. Lett.* **1985**, *54*, 599. (b) Gloux, J.; Gloux, P.; Hendriks, H.; Rius, G. *J. Am. Chem. Soc.* **1987**, *109*, 3220. (c) Gloux, J.; Gloux, P. Second European Inorganic Chemistry Seminar, Wiesbaden, Germany, April 16−20, 1990. (d) Gloux, J.; Gloux, P.; Lamotte, B.; Mouesca, J.-M.; Rius, G. *J. Am. Chem. Soc.* **1994**, *116*, 1953.

(13) Rius, G.; Lamotte, B. *J. Am. Chem. Soc.* **1989**, *111*, 2464.

(14) Mouesca, J.-M.; Rius, G.; Lamotte, B. *J. Am. Chem. Soc.* **1993**, *115*, 4714.

(15) Hagen, K. S.; Watson, A. D.; Holm, R. H. *Inorg. Chem.* **1984**, *23*, 2984.

(16) Berg, J. M.; Hodgson, K. O.; Holm, R. H. *J. Am. Chem. Soc.* **1979**, *101*, 4586.

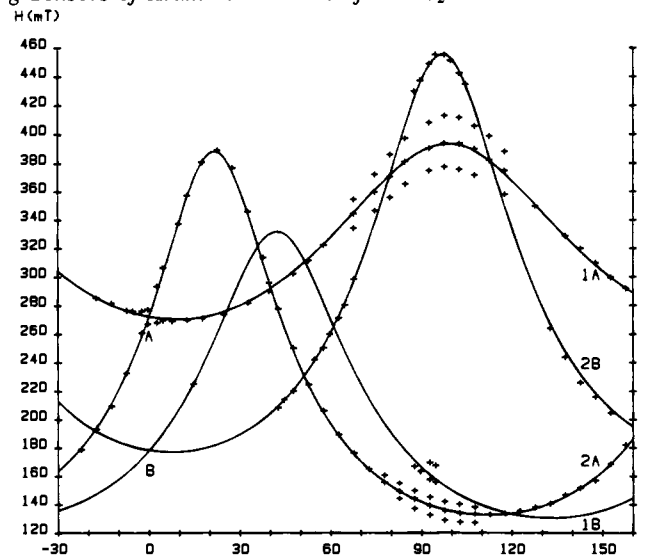

Figure 2. Experimental points and fitted angular variations of the resonance fields for the Kramers doublets A and B in the plane whose normal has direction cosines (−0.598; 0.785; −0.164) in the axis system **a*bc**. The curves are labeled 1 for the EPR site of Table 1 and 2 for the second EPR site. The zero of orientations is set at the intersection of this plane with the plane *ca**, a direction which gives rise to the noncrossing phenomenon for the A data points seen in the figure. It is the direction whose direction cosines are (0.265; 0; −0.964) in **a*bc**, which is approximately 165° from **c** in the plane *ca**. Microwave frequency is 9.234 GHz. The splittings by spin−spin interaction, not considered in the fit, are not shown in the graph of the angular variations.

found beforehand by Laue X-ray diagrams. Another set of angular variations, in a plane that we have identified by the direction cosines of its normal (−0.598; 0.785; −0.164) in the system of orthogonal axes **a*bc**, is given in Figure 2.

In these figures we observe the angular variations of EPR transitions in two Kramers doublets named A and B which will be identified later as being the fundamental and excited Kramers doublets of an effective spin $S = {}^3/_2$. In agreement with the monoclinic symmetry, in each of the planes *a*b* and *bc* we see for each Kramers doublet the lines of two sites symmetrically set around the **b** axis, perpendicular to the glide plane *ca**; only one site is seen in the glide plane for equivalence reasons. The angular variations of doublet A could generally be followed in all planes. The same could not be done for doublet B, which was generally an order of magnitude weaker: for this doublet, the angular variations could be followed only on restricted sectors. The difficulty is greater in the plane *a*b*, where the angular variations of B border on those of doublet A (see Figure 1), leading to uncertainties in the locations of the corresponding lines. It could have been thought that doublet B, being an excited doublet, would be more easily observable at a higher temperature, but the temperature range in which the signals are visible is very limited owing to the fast spin−lattice relaxation due to low-lying excited states resulting from exchange: observations are hindered by the too fast broadening and by the resulting decrease of line amplitude for both doublets. We now analyze the other effects that combine to make it difficult to follow the angular variations, particularly for the less populated doublet B.

In these Kramers doublets of multiplets of spin $> {}^1/_2$ where there is a strong anisotropy of the effective *g* factor, a large anisotropy of the transition probability is also found, which leads to a drastic weakening of the signal amplitude in some orientations. The transition probability is proportional to $\hat{g}_1^2$,

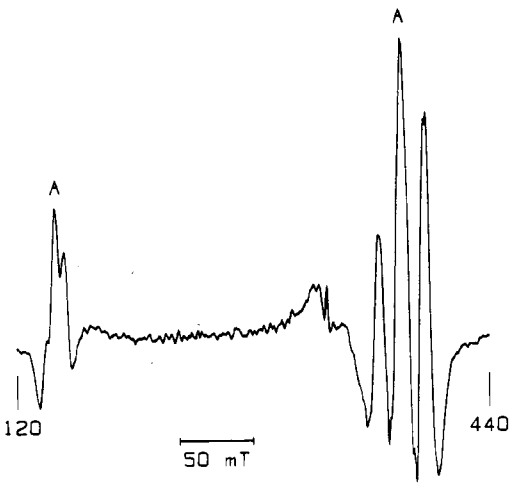

Figure 3. Second derivative of the EPR absorption for **H** in the plane of Figure 2 along the direction having orientation 84.6°. Modulation amplitude is 1 mT and microwave power 10 mW. (The very narrow line at 330 mT, $g = 2$, is isotropic and unrelated to the present study.)

which is given by the classical formula[17]

$$\hat{g}_1^2 = (l_1^2\hat{g}_x^2 + m_1^2\hat{g}_y^2 + n_1^2\hat{g}_z^2) - \hat{g}^{-2}(l_1 l\hat{g}_x^2 + m_1 m\hat{g}_y^2 + n_1 n\hat{g}_z^2)^2 \quad (1)$$

where $\hat{g}_x$, $\hat{g}_y$, and $\hat{g}_z$ are the effective *g* values of the Kramers doublet; l_1, m_1, and n_1 and *l*, *m*, and *n* are the direction cosines of the microwave field $\mathbf{H}_1$ and of the static field **H**, respectively, in the system of axes formed by the principal directions of the effective *g*-tensor; and $\hat{g}$ is the effective *g* factor associated with the direction **H**. With values for $\hat{g}_x$, $\hat{g}_y$, and $\hat{g}_z$ ranging here from 1.4 to more than 5, eq 1 leads to a $\hat{g}_1^2$ and to a transition probability that are both strongly anisotropic.

The high concentration of electron spins in the solid reduces the resolution of the EPR lines. Here we have paramagnetism of all the Fe_4S_4 sites in the $[Fe_4S_4]^+$ form, very different from the case where just a low concentration of spins $[Fe_4S_4]^+$ or $[Fe_4S_4]^{3+}$ is created by γ-irradiation in a diamagnetic crystal with the background Fe_4S_4 sites in the $[Fe_4S_4]^{2+}$ form.[12] The spin−spin interactions between electron spins are then more numerous and stronger, and from this there results a pronounced broadening of the line to the detriment of its amplitude. We find line widths from 10 to 30 mT here, compared to line widths of about 1 mT in the γ-irradiated diamagnetic crystal $(Et_4N)_2[Fe_4S_4(SCH_2Ph)_4]$ for example.[12d]

In some parts of the angular variations of the two doublets, line splittings appear when interactions between electron spins are sufficiently strong to be resolved in spite of the line width. For Kramers doublet B, where the signal amplitude is already small, this splitting restricts even more the range over which the angular variations can be followed. We observe such splittings clearly for Kramers doublet A. They occur as three lines nearly equally spaced both in the *a*b* plane of Figure 1 and in the particular plane of Figure 2, around the turning points of the angular variations of the two sites. Figure 3 shows the spectrum obtained for **H** along a direction of the plane of Figure 2 where such splittings appear for the lines of the two sites for Kramers doublet A. Another type of splitting appears in the *ca** plane of Figure 1: whereas only one site is expected for equivalence reasons, the signal for Kramers doublet A is actually split in two over a large range near the **c** axis. We understand better what happens when we examine the data points near the

(17) Abragam, A.; Bleaney, B. In *Electron Paramagnetic Resonance of Transition Ions*; Oxford University Press: London, 1970.

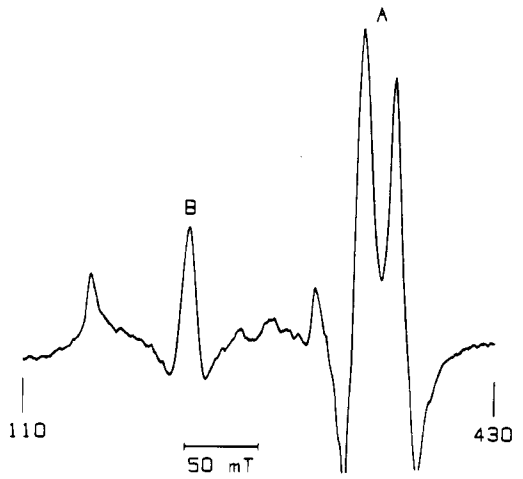

Figure 4. Second derivative of the EPR absorption for **H** in the plane *ca** along the direction having direction cosines (0.109; 0; 0.994) in the axis system **a*bc**, approximately 6° from **c**. Modulation amplitude is 1.25 mT and microwave power 5 mW. (The small extra line at low field, 156 mT, $g = 4.23$, is isotropic and probably corresponds to a spin $S = {}^5/_2$ of adventitious iron.)

c axis in the plane *bc*, as shown in the inset in Figure 2, because the angular variations of two EPR sites which should cross in the **c** direction in fact avoid each other: here we have a phenomenon of noncrossing of the angular variations which results from the noncrossing of energy levels. Figure 4 shows the spectrum obtained for **H** along a direction of the plane *ca** close to **c**, with the splitting of the line corresponding to Kramers doublet A.

All of these splittings arise from the spin−spin interactions $\mathbf{S'}_i\mathbf{J}_{ij}\mathbf{S'}_j$ between the effective electron spins of Kramers doublets of neighboring clusters $[Fe_4S_4]^+$. The noncrossing splittings in some directions of the field **H** where the sites approximate to equivalence give evidence for the presence of crossed coupling terms $S'_{i+}S'_{j-}$ and $S'_{i-}S'_{j+}$ between neighbors in different EPR sites. The threefold splittings have the peculiarity of being simultaneously present for the two sites, and the following relation clearly appears: the local field felt by a site is proportional to the effective g factor of the other site, as it must be when it is the spin−spin interaction between these sites which is the origin of this field, and consequently we observe significantly larger splittings at high field than at low field. Here, when **H** is along a direction **u**, coupling terms $S'_{iu}S'_{ju}$ operate. Such a grouping of three equidistant lines shows the existence of spin−spin couplings of comparable strength between a site and two nearest neighbors in the other type of EPR site; a broader central line and amplitudes that deviate from the ratio 1−2−1 show this equivalence is not quite exact. The shortest iron−iron distances between neighboring clusters are 9.6 Å and, in spite of the spin density delocalization and the large values of the lower field effective g, splittings of 17 mT as attained in the plane of Figure 2 are difficult to explain by only dipolar interactions, without recourse to exchange interactions.

Determination of the Effective *g*-Tensors

1. Spin Hamiltonian. The spin Hamiltonian is composed of two parts

$$H = H_{\text{zero field}} + H_{\text{Zeeman}} = H_{\text{zero field}} + \beta\mathbf{HgS} \qquad (2)$$

where β is the Bohr magneton and **g** is the real g-tensor.

a. Zero Field Hamiltonian. For an effective spin $S = {}^3/_2$

Table 1. Effective g Values and Direction Cosines of the Principal Directions of the g-Tensor of an EPR Site in the Axis System **a*bc**, for Kramers Doublets A and B[a]

doublet	effective g values		direction cosines with respect to a*	b	c
A	1.91	$\mathbf{V}_1$	−0.515	−0.268	−0.814
	5.04	$\mathbf{V}_2$	−0.680	0.706	0.198
	1.41	$\mathbf{V}_3$	0.522	0.656	−0.546
B	1.99	$\mathbf{V}_1$	−0.413	−0.327	−0.850
	1.42	$\mathbf{V}_2$	−0.706	0.704	0.072
	5.19	$\mathbf{V}_3$	0.575	0.630	−0.522

[a] Note that, for doublet A, the powder EPR g values given in ref 7a are 4.96, 1.89, 1.41: the value of the lower field resonance (4.96) is appreciably smaller than our value (5.04). In Figure 3, we can see in the spin−spin splitting of the lower field resonance that the left lateral line is much weaker than the right lateral line. This dissymmetry of the lines in the strong g range will give rise to a shift in the powder spectrum peak, explaining that the apparent g value of ref 7a is too small.

$$H_{\text{zero field}} = \mathbf{SDS} = 2DS_z^2/3 - D({}^1/_3 - \lambda)S_x^2 - D({}^1/_3 + \lambda)S_y^2 \qquad (3)$$

in the system of axes of the principal directions **x**, **y**, and **z** of the tensor **D**, with the rhombicity parameter λ such that $0 \le \lambda \le {}^1/_3$.

b. Zeeman Hamiltonian. If we suppose that the principal axes of the tensor **g** are identical with the principal axes **x**, **y**, and **z** of the tensor **D**, which strictly is only imposed if the paramagnetic center has at least orthorhombic symmetry, we have

$$H_{\text{Zeeman}} = \beta(g_xH_xS_x + g_yH_yS_y + g_zH_zS_z) \qquad (4)$$

Moreover, in first approximation one often assumes $g_x = g_y = g_z = g$ and even that the value of g is 2. Then

$$H_{\text{Zeeman}} = 2\beta\mathbf{HS} \qquad (5)$$

c. Spin Hamiltonian with Effective *g*-Tensor. In the case where the weak-field limit $H_{\text{zero field}} \gg H_{\text{Zeeman}}$ is valid, the problem becomes that of separate Kramers doublets for any half-integer spin, for instance two doublets "$\pm{}^1/_2$" and "$\pm{}^3/_2$" for a spin $S = {}^3/_2$. We can write for any Kramers doublet the spin Hamiltonian

$$H' = \beta\mathbf{H}\hat{\mathbf{g}}\mathbf{S'} \qquad (6)$$

with an effective spin $S' = {}^1/_2$ and an effective g-tensor $\hat{\mathbf{g}}$.

Using the analytic expression of the transition energy which derives from the spin Hamiltonian of eq 6, the angular variations of the transition within doublet A or B were fitted in at least three planes by a least-squares method. The elements of the tensor $\hat{\mathbf{g}}^2$ in the selected system of axes, here the system of axes **a*bc**, are the parameters whose values are given by the fit; after diagonalization, they yield the effective g values and the corresponding principal directions of Table 1.

2. *g*-Tensor of Doublet A. For doublet A, the fit was made to the angular variations in the three perpendicular planes *a*b* and *bc* (with two sites) and *ca** (with one site). Within this framework, an ambiguity has generally to be resolved since a priori there are two ways to connect the curves in the planes with two sites (*a*b* and *bc*). This leads to the two possible sign sets (−+, +−) and (−−, ++) for the corresponding nondiagonal elements $(\hat{g}^2)_{a^*b}$ and $(\hat{g}^2)_{bc}$ of the two sites. Usually, the correct association is selected by the study of the angular variations in a fourth plane appropriately selected. The problem may be simplified when the anisotropy is very strong, as is the

case here: when the nondiagonal elements are very large, it may happen that one of the sets leads to a negative eigenvalue for the tensor $\hat{\mathbf{g}}^2$ and is thus excluded. This happens in the present case, and the association (−−, ++) has to be rejected for this straightforward reason.

The effective g values and the corresponding principal directions of one site of doublet A are given in Table 1. The principal directions are identified by their direction cosines in the system of axes **a*bc**. The other EPR site is obtained by a change of sign of the direction cosines along the axes **a*** and **c**. In Figure 1 we observe a good agreement between the experimental points and the continuous line fit, which allows us to believe that the tensor is obtained with satisfying accuracy. Using the elements of the tensor $\hat{\mathbf{g}}^2$ thus obtained, we have also done least-square fits of the angular variations in general planes where the fitting parameters are the orientation parameters that define, in the system of axes **a*bc**, the general plane and directions in this plane. This has given very acceptable fits, in particular in the case of the fit represented by a continuous line in Figure 2 which leads to the determination of the orientation of the plane studied.

3. g-Tensor of Doublet B. The g-tensor of doublet B is much more difficult to obtain. Measurements in the three crytallographic planes a^*b, bc, and ca^* as in the case of doublet A are not enough. In the plane a^*b the angular variations are too close to those of doublet A (see Figure 1), and because of the relative weakness of the lines of doublet B and the large line widths, doublet B is often hidden by doublet A. A well-resolved line appears for doublet B only near the maximum for the high-field EPR site. Concerning the low-field EPR site, rotating the field in other planes leads to the conclusion that the EPR line is split and the data points which appear clearly above those of doublet A correspond to, unfortunately, only the high-field component of the splitting. In the bc plane, the line corresponding to the low-field site clearly splits in three; in a large sector where **H** approaches **b**, one can no longer observe the signal of either site. The problem of the site assignment of the curves in the planes a^*b and bc can, however, be resolved as before by the rejection of the bad solution that gives a negative eigenvalue for the tensor $\hat{\mathbf{g}}^2$. This leads to an assignment of the high-field branch in one of the planes a^*b and bc and the low-field branch in the other plane being attributed to the same site, as was already the case for doublet A.

Consequently, in the acquisition of the final results we have used other planes, like that of Figure 2. Once the orientation of these supplementary planes has been deduced as described above from fits of the angular variations of doublet A, we combined the data for these additional planes and the basic planes a^*b, bc, and ca^* and we fitted the totality of the angular variations of doublet B to obtain the corresponding tensor $\hat{\mathbf{g}}^2$. The effective g values and the corresponding principal directions of a site of doublet B are given in Table 1, the directions being defined by their direction cosines in the system of axes **a*bc**. We recall that the other EPR site is obtained by a change of sign of the direction cosines along the axes **a*** and **c**. The accuracy obtainable by a fit in the three perpendicular planes when the fitted points are regularly distributed, as was the case for doublet A, cannot be preserved here where we compensate for the strong inhomogeneity of the data point distribution by adding supplementary planes. The effective g-tensor of doublet B reflects the inaccuracy of the determination of the orientation of these supplementary planes.

Analysis of Results

1. Geometric Correlations. Doublet A has already been identified in the powder EPR spectrum by Carney et al.[7a] as being the fundamental Kramers doublet associated with paramagnetism of the cubane Fe_4S_4. We associate doublet B, which has great similarity with doublet A, with the cubane Fe_4S_4 also. The anisotropy of the effective g-tensors of these doublets is such that they can only correspond to an effective spin $S > 1/2$. Then there are two possible cases:

(a) Doublets A and B come from two different spin multiplets.

(b) Doublet B is an excited Kramers doublet and doublet A the fundamental Kramers doublet of the same spin multiplet, the fundamental multiplet associated with the intrinsic cubane Fe_4S_4. We recall that the broadening of lines due to the fast spin−lattice relaxation does not allow detection of the population transfer between doublets A and B which would have to appear in this hypothesis on raising the temperature.

The similarity of the two doublets appears already via very similar effective g values. This is why doublet B is not visible in the powder EPR spectrum: its own singularities are hidden by those of doublet A. The similarity is emphasized by the EPR sites selected in Table 1, in view of the direction cosines of their principal directions in the system of axes **a*bc**. We find two principal axis sets with neighboring orientations, the directions with the same index, $\mathbf{V}_1$, $\mathbf{V}_2$, and $\mathbf{V}_3$, being rotated from each other by angles of 7°, 7°, and 4°, respectively. Then, the feature that differentiates between the sites of Table 1 but at the same time establishes their correlation is that we find in the neighboring principal directions either "opposite" effective g values or intermediate effective g values near $g = 2$. We shall see below that this special correlation between the sites of Table 1 is in agreement with case b above, if we suppose that they correspond to the fundamental and excited doublets of the same multiplet of effective spin $3/2$. The connection of the EPR sites of Table 1 with the same site of the cubane Fe_4S_4 in the crystal is then also justified, which was not obvious a priori. Concretely, this connection causes the angular variations for the same site of A and B to be opposite in Figure 1: when the A line is in high field, the B line is in low field, and vice versa.

The question is then to find which EPR site, the one in Table 1 or the other site, is connected with a given Fe_4S_4 site in the crystal. We use for this comparison the Fe_4S_4 site whose atomic parameters appear in ref 16. This question remains unanswered because a binary point symmetry with axis parallel to **b** links the two EPR sites, on the one hand, and, on the other hand, changes the atomic positions of the cubane Fe_4S_4 like an internal quasi-symmetry.[18] The two EPR sites are thus set in orientations that a priori appear similar compared with a crystal site, and one solution cannot be preferred to the other. More precisely, the orthogonal axis set formed by the three principal directions $\mathbf{V}_1$, $\mathbf{V}_2$, and $\mathbf{V}_3$ of the EPR site of Table 1 is relatively near the quasi-orthogonal set of three directions formed by the bisector of the angle $(\overrightarrow{Fe_3Fe_1}, \overrightarrow{Fe_3Fe_4})$ and the directions $\overrightarrow{Fe_1Fe_4}$ and $\overrightarrow{Fe_2S_2}$ of the Fe_4S_4 site defined in ref 16. In the same way the orthogonal set of directions $\mathbf{V}_1$, $\mathbf{V}_2$, and $\mathbf{V}_3$, of the other EPR site is relatively near the quasi-orthogonal set of directions formed by the bisector of the angle $(\overrightarrow{Fe_4Fe_2}, \overrightarrow{Fe_4Fe_3})$ and the directions $\overrightarrow{Fe_2Fe_3}$ and $\overrightarrow{Fe_1S_1}$. These two groups of crystal directions are given in Table 2 by their direction cosines in the

(18) The "normal to opposite faces of the cubane" $\overrightarrow{Fe_1Fe_2} \times \overrightarrow{Fe_3Fe_4}$ is practically parallel to **b**: in the system of axes **a*bc** it has direction cosines (−0.026; −0.999; −0.043).

Table 2. Comparison between the Principal Directions of the g-Tensor and the Geometry of the Site Fe_4S_4 of Ref 16, for the Two EPR Sites of Each Kramers Doublet[a]

	direction cosines with respect to			angle (deg) with V direction of		
	a*	b	c	center A	center B	V direction
bisector[b]	−0.680	−0.367	−0.635	15	20	V_1[d]
$\overrightarrow{Fe_1Fe_4}$	−0.650	0.714	0.258	4	11	V_2[d]
$\overrightarrow{Fe_2S_2}$	0.351	0.590	−0.727	15	18	V_3[d]
bisector[c]	0.652	−0.447	0.613	17	20	V_1[e]
$\overrightarrow{Fe_2Fe_3}$	0.685	0.691	−0.231	2	9	V_2[e]
$\overrightarrow{Fe_1S_1}$	−0.322	0.565	0.760	17	20	V_3[e]

[a] The interatomic directions for the site Fe_4S_4 of ref 16 are given by their direction cosines in the axis system **a*bc**, and their angle with the neighboring direction V_1 or V_2 or V_3 is specified. [b] Of ($\overrightarrow{Fe_3Fe_1}$, $\overrightarrow{Fe_3Fe_4}$). [c] Of ($\overrightarrow{Fe_4Fe_2}$, $\overrightarrow{Fe_4Fe_3}$). [d] Of EPR site of Table 1. [e] Of second EPR site.

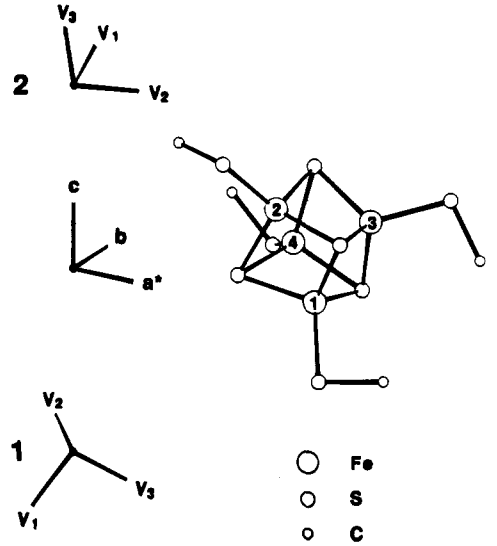

Figure 5. Orientation of the principal axis sets for the two EPR sites of Kramers doublet A and the system of axes **a*bc** in relation to the structure of the $Fe_4S_8C_4$ portion of the $[Fe_4S_4(SCH_2Ph)_4]^{3-}$ anion site defined in ref 16. The principal axis sets are labeled 1 for the EPR site of Table 1 and 2 for the second EPR site.

system of axes **a*bc**, as calculated from the crystallographic data,[16] and we specify their angle with the neighboring direction V_1 or V_2 or V_3 of the concerned EPR site, for doublets A and B. We notice that the direction V_2 is particularly close to the iron−iron direction. The orientation of the principal axis sets for the two EPR sites of Kramers doublet A and the system of axes **a*bc** in relation to the structure of the $Fe_4S_8C_4$ portion of the $[Fe_4S_4(SCH_2Ph)_4]^{3-}$ anion site defined in ref 16 are shown in Figure 5.

2. Connection between the Doublets. (a) If eq 5 is an adequate approximation of the Zeeman Hamiltonian, the effective g values $\hat{g}_x$, $\hat{g}_y$, and $\hat{g}_z$ of each doublet depend only on λ, according to well-known diagrams.[19] The tensor **D** and the effective g-tensors $\hat{\mathbf{g}}_{1/2}$ and $\hat{\mathbf{g}}_{3/2}$ of two doublets have the same principal directions **x**, **y**, and **z** in common. In the borderline case of $\lambda = 1/3$, the effective g values of the doublets are equal two by two so that

$$(\hat{g}_{1/2})_x = (\hat{g}_{3/2})_x = 2$$
$$(\hat{g}_{1/2})_y = (\hat{g}_{3/2})_z = 5.46 \qquad (7)$$
$$(\hat{g}_{1/2})_z = (\hat{g}_{3/2})_y = 1.46$$

We find in this association between the effective g values and the principal directions the same kind of correlations as those connecting the effective g-tensors of sites of doublets A and B of Table 1.

(b) While still remaining in the borderline case $\lambda = 1/3$, we can give more freedom to the Zeeman Hamiltonian by using the approximate form eq 4. The real g values g_x, g_y, and g_z can now be different from 2 and unequal. From Pilbrow,[20] the relations between the absolute values of the effective g values and of the real g values are written

$$(\hat{g}_{1/2})_x = (\hat{g}_{3/2})_x = g_x$$
$$(\hat{g}_{1/2})_y = (1+\sqrt{3})g_y \qquad (\hat{g}_{3/2})_z = (1+\sqrt{3})g_z \qquad (8)$$
$$(\hat{g}_{1/2})_z = (\sqrt{3}-1)g_z \qquad (\hat{g}_{3/2})_y = (\sqrt{3}-1)g_y$$

If, for instance, $g_x = 1.95$, $g_y = 1.85$, and $g_z = 1.90$, we have

$$(\hat{g}_{1/2})_x = 1.95 \qquad (\hat{g}_{3/2})_x = 1.95$$
$$(\hat{g}_{1/2})_y = 5.04 \qquad (\hat{g}_{3/2})_z = 5.19 \qquad (9)$$
$$(\hat{g}_{1/2})_z = 1.39 \qquad (\hat{g}_{3/2})_y = 1.36$$

values which compare well with the effective g values of doublets A and B

$$(\hat{g}_A)_1 = 1.91 \qquad (\hat{g}_B)_1 = 1.99$$
$$(\hat{g}_A)_2 = 5.04 \qquad (\hat{g}_B)_3 = 5.19 \qquad (10)$$
$$(\hat{g}_A)_3 = 1.41 \qquad (\hat{g}_B)_2 = 1.42$$

Doublet A, the fundamental, has to be associated with doublet "$\pm 1/2$", and doublet B with doublet "$\pm 3/2$", a situation that corresponds to $D > 0$. Exchange of values between g_y and g_z leads also to exchange of the effective g values of the effective g-tensors $\hat{\mathbf{g}}_{1/2}$ and $\hat{\mathbf{g}}_{3/2}$ in the same line, and fundamental doublet A has now to be associated with doublet "$\pm 3/2$" and doublet B with doublet "$\pm 1/2$", a situation that corresponds to $D < 0$. At this stage, and whatever the sign of D may be, we want to emphasize that the tensors of Table 1 are in sufficiently close correspondence with the theoretical tensors that we can identify doublets A and B as fundamental and excited doublets of an effective spin 3/2 whose Zeeman Hamiltonian is not too different from the approximate form of eq 4 in the borderline case $\lambda = 1/3$.

(c) In fact, the orthorhombic symmetry approximation to the Zeeman Hamiltonian given by eq 4 is not fulfilled, because this iron−sulfur cubane has really no exact symmetry. Strictly, there is no reason why the real g-tensor **g** should have the same principal directions as those of the tensor **D**. Nor are the effective g-tensors of the two Kramers doublets required to have the same principal directions as each other, and this appears moreover from the comparison of their principal directions made above. The relations 8 between the effective and real g values which derive from eq 4 are also no longer strictly valid; this justifies the differences found above between the theoretical and experimental effective g values.

(d) Carney et al. found that the three effective g values of the fundamental doublet which they obtained by powder EPR

(19) (a) Maltempo, M. M. *Chem. Phys. Lett.* **1979**, *60*, 441. (b) Lindahl, P. A.; Day, E. P.; Kent, T. A.; Orme-Johnson, W. H.; Münck, E. *J. Biol. Chem.* **1985**, *260*, 11160. (c) Hagen, W. R. In *Advances in Inorganic Chemistry*; Sykes, A. G., Ed.; Academic Press: New York, 1992; Vol. 38, p 165.

(20) Pilbrow, J. R. *J. Magn. Reson.* **1978**, *31*, 479.

could not be inserted in the classical diagrams giving $\hat{g}_x$, $\hat{g}_y$, and $\hat{g}_z$ in terms of λ under the approximation for the Zeeman Hamiltonian given by eq 5 with $g = 2$.[7a] In the analysis that we developed above, we have simply introduced a deviation of real g values from $g = 2$ and we have noted that one must also take account of a quite different aspect, the low symmetry of the species. We have proposed a grouping of g values around $g_{av} = 1.9$. This deviation of real g values from $g = 2$ of course implies that the effective spin $S = {}^3/_2$ being investigated results from some mixture of a pure spin state $S = {}^3/_2$ with other pure spin states, but it is perhaps going rather far to consider it as a quantum mixture[21] of pure spins $S =$ "$^3/_2 + {}^1/_2$" as suggested by Carney et al.[7] In contrast, the ground spin states $S = {}^1/_2$ found in other cubanes 4Fe-4S belong as a general rule to the $g_{av} = 1.94$ type and are considered as pure spins.[7a]

3. g-Tensors and Resonance Models. Within the framework of models of the reduced 4Fe-4S $[Fe_4S_4]^+$, Noodleman[22] starts with the Heisenberg Hamiltonian with two parameters[10]

$$H = J_1(\mathbf{S_K} + \mathbf{S_L} + \mathbf{S_M})\mathbf{S_N} + J_2(\mathbf{S_K}\mathbf{S_L} + \mathbf{S_L}\mathbf{S_M} + \mathbf{S_M}\mathbf{S_K}) \quad (11)$$

where $J_1 = J_{Fe^{3+}-Fe^{2+}}$ and $J_2 = J_{Fe^{2+}-Fe^{2+}}$. Noodleman supposes that there also exists a double-exchange interaction of the form $\pm B(S_{MN} + {}^1/_2)$ between the eigenstates of this Hamiltonian, where the iron 3+ is in position N, and the eigenstates of the Hamiltonian of the same type where the iron 3+ is in position M, i.e. within a specific mixed-valence pair having spin S_{MN}. In this model, total spin states $S = {}^1/_2$ are favored as fundamental rather than total spin states $S = {}^3/_2$.[8]

Really, it is by introducing a second interaction of double exchange that Noodleman and Case[8] find a spin $^3/_2$ multiplet as ground state. The energies in terms of the total spin S, except for a constant independent of spin, are given by

$$E(S) = JS(S+1)/2 \pm B(S_{MN} + {}^1/_2) \pm B'(S + {}^1/_2) \quad (12)$$

To the resonance term of the mixed-valence pair (M,N) is added a resonance term that connects this mixed-valence pair (M,N) and the pair (K,L) of 2+ irons. Here, the problem is simplified by reducing the Heisenberg Hamiltonian to only one J parameter, because distinguishing two parameters J_1 and J_2 has only minor importance in the stabilization of spin $^3/_2$ compared with the introduction of the coupling B'.[8]

D_{2d} symmetry, which is consistent with the existence of the two couplings B and B' that induce a spin $^3/_2$, would give axial tensors around a "normal to opposite faces of the cubane", i.e. a direction perpendicular to two iron−iron directions. The experimental effective g-tensors show no trace of this, since the deviation from axiality is even a maximum (λ parameter $\cong {}^1/_3$). Besides, we shall see below that there is no g-tensor principal direction normal to opposite faces of the cubane.

In the case of the $S = {}^1/_2$ spins associated with the reduced forms $[Fe_4S_4]^+$ that are created by γ-irradiation in the compounds $[Fe_4S_4]^{2+}$, we found that a principal direction of the g-tensor, the one belonging to the largest g value, was near a normal to opposite faces of the cubane.[12] This led us to consider a B resonance in relation with a twofold symmetry around the normal considered. Here, the only principal direction not too far from a normal to opposite faces of the cubane, $\mathbf{V_1}$, is already about 20° away from $\overrightarrow{Fe_1Fe_4} \times \overrightarrow{Fe_2Fe_3}$ (21° for $\mathbf{V_1}$ of EPR site of Table 1, 19° for $\mathbf{V_1}$ of second EPR site, for both Kramers doublets).

One feature that might be an indication of symmetry is the nearness of the directions $\mathbf{V_2}$ to an iron−iron direction ($\mathbf{V_2}$ of EPR site of Table 1 with Fe_1Fe_4 or $\mathbf{V_2}$ of the second EPR site with Fe_2Fe_3, see Table 2). This would allow the median plane as a possible symmetry plane, but this plane is not one of the planes of the C_{2v} idealized symmetry which is given in ref 16 for this cubane, with the normal $\overrightarrow{Fe_1Fe_3} \times \overrightarrow{Fe_2Fe_4}$ as twofold axis.

Thus, the behavior of the effective g-tensors is not really conclusive. We do not find clearly any symmetry aspects consistent with an equivalence of all four irons (case of two strong resonance couplings B and B') nor even with an equivalence of the irons only in pairs (case of only one strong resonance coupling B).[23] But, as emphasized in the referees' comments on this paper, one cannot for all that come to the conclusion that there is no resonance: a small symmetry-lowering perturbation of no consequence for resonance might in contrast have a large effect on the tensors if the excited state that mixes with the ground state is not too far away.

Conclusion

After a single-crystal EPR study of the effective spin $S = {}^3/_2$ ground state of the $[Fe_4S_4]^+$ ion of the compound $(Et_4N)_3[Fe_4S_4(SCH_2Ph)_4]$, which has allowed us to follow the angular variations of the transitions associated with the two Kramers doublets, we have shown that the effective g-tensors of these Kramers doublets have principal g values and directions that can be explained by a nonaxial zero field splitting tensor ($\lambda \cong {}^1/_3$) and by g values of the real g-tensor around $g_{av} = 1.9$.

We have seen that it is difficult to insert these results in the framework of the theories of electron delocalization and strong double exchange. This single-crystal study is the first of the kind for an intrinsic spin in the 4Fe-4S compounds, and we should be able to improve our understanding by examining other compounds of the family having effective spin $S = {}^3/_2$.

Acknowledgment. We are grateful to Ronald Cox for helpful comments. We thank Jean Laugier and Joël Moulin for the Laue X-ray diagrams, and we are indebted to Gérard Desfonds for technical assistance.

JA943995S

(21) A quantum mixture of pure spin states refers to a situation in which *substantial* contributions of two or more pure spin states exist, i.e. a situation which goes beyond the treatment of the spin−orbit coupling as small second-order terms in perturbation theory (see: Maltempo, M. M. *J. Chem. Phys.* **1974**, *61*, 2540).

(22) (a) Noodleman, L. *Inorg. Chem.* **1991**, *30*, 246. (b) Noodleman, L. *Inorg. Chem.* **1991**, *30*, 256.

(23) Mössbauer results of ref 7a would agree with equivalence of the irons in pairs.